# Effects of sulfate coatings on the ice nucleation properties of a biological ice nucleus and several types of minerals

Donna I. Chernoff[1] and Allan K. Bertram[1]

Received 24 March 2010; revised 17 June 2010; accepted 28 June 2010; published 21 October 2010.

[1] An optical microscope coupled to a flow cell was used to study the ice nucleation properties of uncoated and coated mineral dust and SNOMAX (a proxy for biological ice nucleators made from cells of *Pseudomonas syringae*) at temperatures ranging from 234 to 247 K. We define the onset conditions as the relative humidity (RH) and temperature at which the first ice nucleation event was observed. The results show that $H_2SO_4$ coatings modified the ice nucleation properties of all the minerals studied. For kaolinite and illite, the acid coatings increased the RH over ice ($RH_i$) required for ice nucleation by ~30% $RH_i$; for montmorillonite and quartz, the acid coatings increased the $RH_i$ by ~20% $RH_i$. $NH_4HSO_4$ coatings also influenced the ice nucleation properties of kaolinite particles. In addition, our results indicate that SNOMAX is a reasonably good ice nucleus, having onset values between 110 to 120% $RH_i$. In contrast to the mineral studies, sulfuric acid coatings did not hinder the ice nucleating ability of SNOMAX particles. Combined, our results support the idea that anthropogenic emissions of $SO_2$ and $NH_3$ may influence the ice-nucleating properties of mineral dust particles. From our laboratory data, we also determined contact angles ($\theta$) between the heterogeneous nuclei and ice embryos according to classical nucleation theory to parameterize the laboratory data for inclusion in atmospheric models. The data show that for uncoated ice nuclei the contact angles are small (below ~20°), but for mineral particles coated with sulfuric acid, the contact angles are larger (above ~60°).

**Citation:** Chernoff, D. I., and A. K. Bertram (2010), Effects of sulfate coatings on the ice nucleation properties of a biological ice nucleus and several types of minerals, *J. Geophys. Res.*, *115*, D20205, doi:10.1029/2010JD014254.

## 1. Introduction

[2] Aerosol particles are abundant in the atmosphere, and these aerosol particles can indirectly influence climate by modifying the formation conditions and properties of ice clouds and mixed-phase clouds. To better understand this important topic, an improved understanding of the ice nucleation properties of atmospheric aerosols is required, and these properties need to be parameterized and incorporated into climate models [*Baker and Peter*, 2008; *Cantrell and Heymsfield*, 2005; *Hegg and Baker*, 2009; *Houghton*, 2001].

[3] Ice nucleation may occur in the atmosphere either homogeneously or heterogeneously. Homogeneous nucleation involves the spontaneous freezing of liquid droplets. In heterogeneous nucleation, ice forms on an insoluble or partially soluble aerosol particle.

[4] Mineral dust particles are abundant in the atmosphere, and both laboratory and field studies have shown that mineral dust particles are effective heterogeneous ice nuclei (IN). Laboratory studies indicate that mineral dust particles can lower the supersaturation required for ice formation compared to homogeneous nucleation. Field measurements have shown that these particles can have a significant effect on cloud formation and cloud properties [*DeMott et al.*, 2003; *Sassen*, 2002; *Sassen et al.*, 2003]. Measurements have also shown that the cores of ice crystals often contain mineral dust inclusions, indicating that these particles play an important role in atmospheric ice formation [*Cziczo et al.*, 2004; *Heintzenberg et al.*, 1996; *Twohy and Poellot*, 2005].

[5] While in the atmosphere, mineral dust particles can be coated with organic and inorganic material [*Hinz et al.*, 2005; *McNaughton et al.*, 2009; *Sullivan et al.*, 2007; *Usher et al.*, 2003; *Wiacek and Peter*, 2009]. These coatings may affect the ice nucleation properties of mineral dust [*Gallavardin et al.*, 2008; *Phillips et al.*, 2008]. Nevertheless, there have only been a few studies that have directly compared the ice-nucleating ability of uncoated and coated mineral dust particles at atmospherically relevant conditions [*Archuleta et al.*, 2005; *Cziczo et al.*, 2009; *Eastwood et al.*, 2009; *Gallavardin et al.*, 2008; *Kanji et al.*, 2008; *Knopf and Koop*, 2006; *Möhler et al.*, 2008a; 2008c; *Salam et al.*, 2007]. A few other studies have measured the freezing properties of aqueous inorganic or organic solution droplets containing mineral dust particles [*Ettner et al.*, 2004; *Hung et al.*, 2003; *Koop and Zobrist*, 2009; *Zobrist et al.*, 2008; *Zuberi et al.*, 2002].

[6] Recently, we showed that sulfuric acid coatings (ammonium-to-sulfate ratio (ASR) = 0) can have a significant

[1]Department of Chemistry, University of British Columbia, Vancouver, British Columbia, Canada.


0148-0227/10/2010JD014254

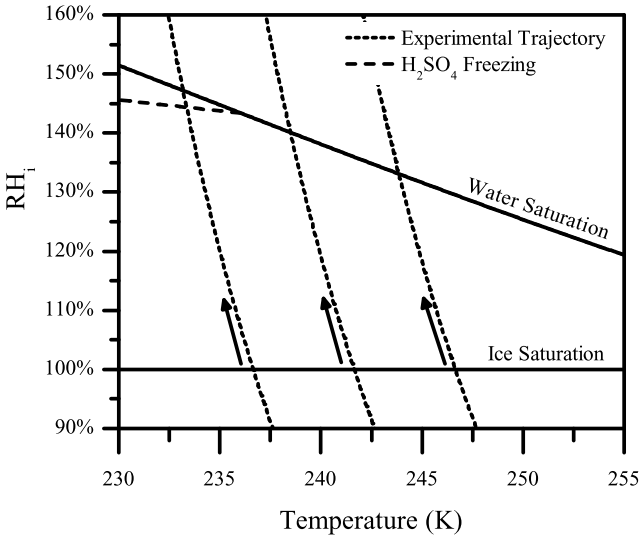


**Figure 1.** Typical experimental trajectories. The temperature was reduced at a rate of 0.1 K min$^{-1}$ while the water vapor partial pressure was held constant. The trajectories correspond to ice frost points of 237, 242, and 247 K, where the ice frost point is defined as the temperature at which the relative humidity over ice ($RH_i$) = 100%. Trajectories were calculated using the saturation vapor pressures of water and ice from the parameterization of *Murphy and Koop* [2005]. The dashed line represents the threshold for homogeneous freezing of sulfuric acid droplets 8 $\mu$m in diameter at a freezing rate of 10 s$^{-1}$ [*Koop et al.*, 2000].

effect on the ice nucleation properties of kaolinite particles [*Eastwood et al.*, 2009]. Kaolinite particles can make up ~5–10% of mineral dust mass [*Glaccum and Prospero*, 1980]. In this previous study, we showed that a sulfuric acid coating on kaolinite particles increased the relative humidity over ice ($RH_i$) required for ice nucleation compared to uncoated particles by ~30%, consistent with recent results on Arizona test dust (ATD) and illite [*Möhler et al.*, 2008c]. We also looked at the effect of ammonium sulfate coatings (ASR = 2) on kaolinite. These coatings had a different effect from sulfuric acid coatings. At the coldest temperature studied (236 K), the ammonium sulfate-coated particles were as efficient as the uncoated kaolinite particles, whereas at the warmer temperatures (240 and 245 K) the onset $RH_i$ values were significantly higher than the uncoated case. These results suggest that the ASR of the coating is important, at least for certain sizes.

[7] In addition to mineral dust, biological particles may play an important role in the formation of ice clouds in the atmosphere [*Ariya et al.*, 2009; *Christner et al.*, 2008a; *Christner et al.*, 2008b; *Möhler et al.*, 2007; *Phillips et al.*, 2009; *Szyrmer and Zawadzki*, 1997]. In particular, the bacteria *Pseudomonas syringae* has been identified as an extremely efficient IN, demonstrating ice-nucleating activity at temperatures as warm as –2°C in purified samples [*Möhler et al.*, 2007]. However, the abundance of biological particles in the atmosphere and their activity under atmospheric conditions remain poorly understood. The potential role of biological particles in atmospheric ice formation has recently been emphasized in field studies done in Wyoming and the Amazon basin [*Pratt et al.*, 2009; *Prenni et al.*, 2009]. In both studies, the ice nuclei composition was dominated by mineral dust and biological particles.

[8] Similar to mineral dust, biological particles can also be coated with inorganic and organic material in the atmosphere [*DeMott et al.*, 2003; *Lammel et al.*, 2005]. We are not aware of any studies in which the ice nucleation properties of uncoated and coated biological particles were directly compared. Studies have investigated the freezing of dilute aqueous solutions [*Chen et al.*, 2002; *Kawahara et al.*, 1996; *Kawahara et al.*, 1995; *Obata et al.*, 1993; *Pouleur et al.*, 1992; *Yin et al.*, 2005] and concentrated aqueous solutions [*Koop and Zobrist*, 2009] containing biological particles.

[9] In the following sections, we expand on our previous work [*Eastwood et al.*, 2009] and consider other mineral dusts which have been shown to be abundant in the atmosphere [*Chester et al.*, 1972; *Glaccum and Prospero*, 1980; *Usher et al.*, 2003], as well as a more complete range of sulfate coatings. The ice nucleation properties of SNOMAX, a proxy for biological ice nucleators, are also investigated. SNOMAX is produced from cells of *P. syringae* that have been grown under optimal conditions to maximize ice nucleation. We interpret our results using classical nucleation theory. The results from this study should prove useful for understanding the effects of anthropogenic emissions of $SO_2$ and $NH_3$ on climate by influencing the ice-nucleating properties of mineral dust and biological particles.

## 2. Experimental

### 2.1. Ice Nucleation Measurements

[10] The apparatus used in these studies has been described in detail previously [*Dymarska et al.*, 2006; *Parsons et al.*, 2004]. The apparatus consisted of an optical microscope coupled to a flow cell in which the relative humidity could be accurately controlled. In a typical experiment, mineral dust or SNOMAX particles (coated or uncoated) were deposited on the bottom surface of the flow cell, the $RH_i$ inside the cell was increased, and the conditions under which ice first formed were determined with a reflected light microscope. The bottom surface of the flow cell, which supported the particles, consisted of a glass coverslide treated with dichlorodimethylsilane to make a hydrophobic layer, which reduced the probability of ice nucleation directly on the surface. Typical experimental $RH_i$ trajectories used in our experiments are illustrated in Figure 1. The three trajectories correspond to ice frost points of 237, 242, and 247 K, where the ice frost point is defined as the temperature at which the $RH_i$ = 100%. Included in this figure is the threshold for homogeneous freezing of sulfuric acid droplets 8 $\mu$m in diameter at a freezing rate of 10 s$^{-1}$ [*Koop et al.*, 2000]. At the beginning of the experiments, the particles were exposed to a flow of dry He gas ($RH_i$ <1%) at room temperature. Next, the temperature of the cell was rapidly lowered and the $RH_i$ was set to ~80%. The nucleation experiments were then conducted by steadily decreasing the temperature and increasing the $RH_i$. The $RH_i$ ramp rate was ~1% min$^{-1}$. In a previous study in our group, experiments were carried out using a ramp rate of ~0.5% min$^{-1}$. No difference in results was obtained, suggesting the aqueous coatings were in equilibrium with the water vapor [*Eastwood et al.*, 2009]. Growth rate calculations of aqueous solution droplets have also been done in our group using the equations presented by

**Table 1.** Chemical Formulae of the Four Minerals Studied

| Mineral | Formula |
|---|---|
| Kaolinite | $Al_4Si_4O_{10}(OH)_8$ |
| Illite | $(K,H_3O)(Al,Mg,Fe)_2(Si,Al)_4O_{10}[(OH)_2,H_2O]$ |
| Montmorillonite | $(Na,Ca)_{0.33}(Al,Mg)_2Si_4O_{10}(OH)_2{\cdot}nH_2O$ |
| Quartz | $SiO_2$ |

*Pruppacher* [1997] to further confirm that the sulfuric coatings were in equilibrium with the gas-phase water vapor in our experiments. The uncertainty in our measurements due to nonequilibrium conditions is at most 3% $RH_i$ [*Eastwood et al.*, 2009].

### 2.2. Sample Preparation and Thickness of the Coatings

[11] The mineral dusts used in this study are listed in Table 1 along with their chemical formulae. Kaolinite and montmorillonite were purchased from Fluka, illite was provided by the Clay Minerals Society, and quartz was obtained from U.S. Silica. SNOMAX was purchased from York Snow, Inc. As mentioned, SNOMAX is produced from cells of *P. syringae* that have been grown under optimal conditions to maximize ice nucleation frequency. The cells are then concentrated using ultrafiltration and frozen into pellets. Next the pellets are freeze-dried and exposed to beta irradiation to make a sterile product [*Lee et al.*, 1995]. Note that although SNOMAX is made from cells of *P. syringae*, it does not display the same freezing spectrum (fraction frozen vs. temperature) as some naturally occurring strains of *P. syringae*. Also note that the freezing spectrum of naturally occurring *P. syringae* can vary significantly from strain to strain [*Gross et al.*, 1983; *Hirano et al.*, 1985; *Möhler et al.*, 2008b; *Ward and DeMott*, 1989].

[12] Coated particles were prepared by mixing the minerals or SNOMAX with the coating material in high-purity water to create a suspension. The composition of the suspension was 1 wt% mineral or SNOMAX and 0.2 wt% coating material. This suspension was placed into an ultrasonic bath for 10 min and then stirred for approximately 2 to 4 days to ensure that the coating material had adequate time to interact with the heterogeneous IN. To deposit the particles on the glass slide, the suspension was passed through a nebulizer using high-purity nitrogen ($N_2$) as a carrier gas. The flow from the nebulizer was directed at a hydrophobic glass slide, and droplets containing the particles were deposited on the surface of the slide upon impaction. Water then evaporated, leaving behind the coated particles. Coated particles produced by this method had an average weight fraction of $H_2SO_4$ or $NH_4HSO_4$ of 0.167 under dry conditions.

[13] Uncoated illite, quartz, and SNOMAX particles were prepared using a procedure similar to that described above. First, these minerals or SNOMAX particles were mixed in high-purity water (composition was 1 wt% mineral or SNOMAX) to create a suspension. The suspension was then placed in an ultrasonic bath for 10 min and then stirred for 2 to 4 days to be consistent with the experimental procedure for the coating experiments. These suspensions were then nebulized, creating droplets on the hydrophobic slides. Water then evaporated, leaving behind the uncoated particles.

[14] For uncoated kaolinite and montmorillonite, we use the results previously published by our group [*Eastwood et al.*, 2008; *Eastwood et al.*, 2009]. In these previous experiments, uncoated kaolinite was suspended in water and then nebulized as described above. For montmorillonite, the particles were produced by dry dispersion. This involved placing the dry particles in a glass vessel immersed in an ultrasonic bath and a flow of ultra-high-purity $N_2$ was passed through the glass vessel to entrain the particles. The flow was then directed at the hydrophobic glass slide, and the particles were deposited on the slide by impaction.

[15] The thickness of the coatings in our experiments was estimated on the basis of the compositions of the starting suspensions and assuming a spherical core shell model (e.g., a kaolinite core surrounded by a uniform $H_2SO_4$ or $NH_4HSO_4$ coating). According to our calculations, under dry conditions (<1% $RH_i$), a kaolinite core with a diameter of 15 $\mu$m will have a 0.7-$\mu$m-thick coating, and a 5 $\mu$m core will have a coating of 0.2 $\mu$m. A coating of 0.2 $\mu$m represents at least a few hundred sulfate layers covering the surface of the particle.

[16] Previously in our group, the thickness of the coatings on kaolinite particles (using the same technique for particle production as discussed above) was further characterized by monitoring the change in particle size as the relative humidity with respect to water ($RH_w$) was increased from <1% to 95% [*Eastwood et al.*, 2009]. From the change in size, we estimated the total amount of water adsorbed when cycling between <1% and 95% $RH_w$ using the thermodynamic model of *Clegg et al.* [1998]. From this, we estimated the amount of $H_2SO_4$ on each particle and, in turn, the thickness of the $H_2SO_4$ coating under dry conditions. Measurements made for 15 individual particles yielded an average weight fraction for the coating of 0.12 ± 0.07 under dry conditions. The uncertainty in this value derives from the uncertainty in the relative humidity measurements.

[17] Two different types of nebulizers were used in our studies. For the minerals we used an in-house design. This resulted in average particle sizes ranging from 6–10 $\mu$m. For the SNOMAX particles, we also used this in-house design, average sizes ranging from approximately 16 to 23 $\mu$m. To generate smaller SNOMAX particles we used a commercially available design (Meinhard Glass Products, Model Number TR-30-A1). The commercial nebulizer generated SNOMAX particles with average sizes of ~6–7 $\mu$m. Note that the SNOMAX particles considered in our studies are most likely agglomerates of several SNOMAX cells, which are typically 1–2 $\mu$m, and/or cell fragments. See the next section for more details on particle size distributions used in the experiments.

### 2.3. Particle Number, Particle Sizes, and Total Surface Area

[18] In typical freezing experiments, a sample held between 100 and 1000 individual particles. Hence, our results correspond to when 0.1 to 1% of the particles nucleated ice. The total surface area of mineral dust or SNOMAX deposited in any particular experiment ranged from $2 \times 10^{-5}$ to $3 \times 10^{-3}$ $cm^2$. The mean diameters and standard deviations for all particle types considered in this study are presented in Table 2.

## 3. Results and Discussion

### 3.1. Effect of Sulfuric Acid Coatings on the Ice Nucleation Properties of Different Minerals

[19] Shown in Figure 2 are the results for uncoated and sulfuric acid coated kaolinite, illite, montmorillonite, and

**Table 2.** Particle Sizes and Standard Deviations for the Mineral Dust and SNOMAX Particles Studied

| Sample | Coating | Size ($\mu$m) | Standard Deviation |
|---|---|---|---|
| Kaolinite | None | 7.7 | 5.3 |
| Kaolinite | $H_2SO_4$ | 7.8 | 5.7 |
| Kaolinite | $NH_4HSO_4$ | 10.3 | 7.2 |
| Kaolinite | $(NH_4)_2SO_4$ | 6.9 | 5.0 |
| Illite | None | 5.9 | 3.8 |
| Illite | $H_2SO_4$ | 7.2 | 5.2 |
| Montmorillonite | None | 8.1 | – |
| Montmorillonite | $H_2SO_4$ | 7.7 | 3.8 |
| Quartz | None | 8.2 | 4.8 |
| Quartz | $H_2SO_4$ | 10.1 | 6.5 |
| SNOMAX[a] | None | 5.8 | 3.7 |
| SNOMAX[a] | $H_2SO_4$ | 6.6 | 5.1 |
| SNOMAX | None | 15.9 | 8.9 |
| SNOMAX | $H_2SO_4$ | 22.8 | 15.6 |

[a]These particles were deposited using a commercially available nebulizer; all other particles were deposited using an in-house made nebulizer.

quartz particles. Each data point corresponds to one freezing event, and the error bars represent the uncertainty in measuring the frost point and temperature at the onset. All experiments were carried out with an ice frost point of 237 K. Included is the $RH_i$ at which liquid water saturation occurs for this experimental trajectory. The $RH_i$ necessary for water saturation was determined by calculating the $RH_i$ at which the experimental trajectory crosses the water saturation line in Figure 1. Also included in Figure 2 is the threshold for homogeneous freezing of sulfuric acid droplets. This threshold was determined by calculating the $RH_i$ at which the experimental trajectory crosses the homogeneous freezing line for sulfuric acid in Figure 1. As mentioned above, the data for kaolinite (uncoated and coated) and montmorillonite (uncoated) are taken from *Eastwood et al.* [2009] and *Eastwood et al.* [2008], respectively, and are plotted here again for comparison purposes. All other data were obtained during this study. The total surface area in any particular experiment ranged from approximately $2 \times 10^{-5}$ to $3 \times 10^{-3}$ $cm^2$. Over this relatively narrow range, the onset results did not depend strongly on the surface area, so we combined the data and compared the averages and the 95% confidence intervals for the coated and uncoated cases in Figure 3. The data show that, for kaolinite and illite, the coatings have a major impact on the $RH_i$ required for ice nucleation; the coating increased the onset $RH_i$ value by ~30%. The effect for montmorillonite and quartz is smaller; in this case, the increase in onset $RH_i$ is ~20%, but there is still a statistically significant effect. It is interesting to note that for kaolinite, montmorillonite, and quartz the average onset values fall below water saturation and the conditions

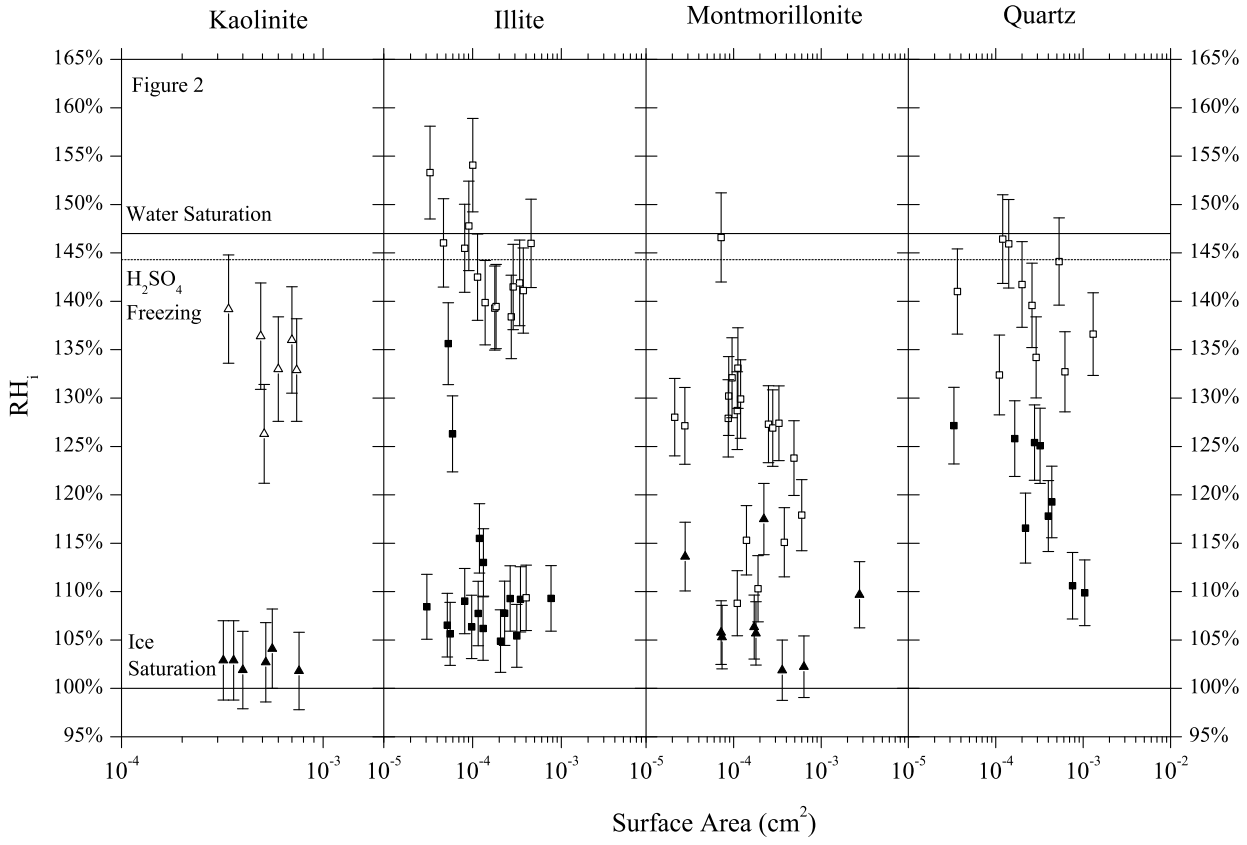


**Figure 2.** Ice nucleation measurements on uncoated (closed symbols) and $H_2SO_4$ coated (open symbols) kaolinite, illite, montmorillonite, and quartz particles. Data are plotted as onset $RH_i$ against surface area ($cm^2$). All experiments were done at an ice frost point of 237 K. Kaolinite results are taken from *Eastwood et al.* [2009]; uncoated montmorillonite results are taken from *Eastwood et al.* [2008]. The dashed line represents the threshold for homogeneous freezing of sulfuric acid droplets 8 $\mu$m in diameter at a freezing rate of 10 $s^{-1}$ [*Koop et al.*, 2000].

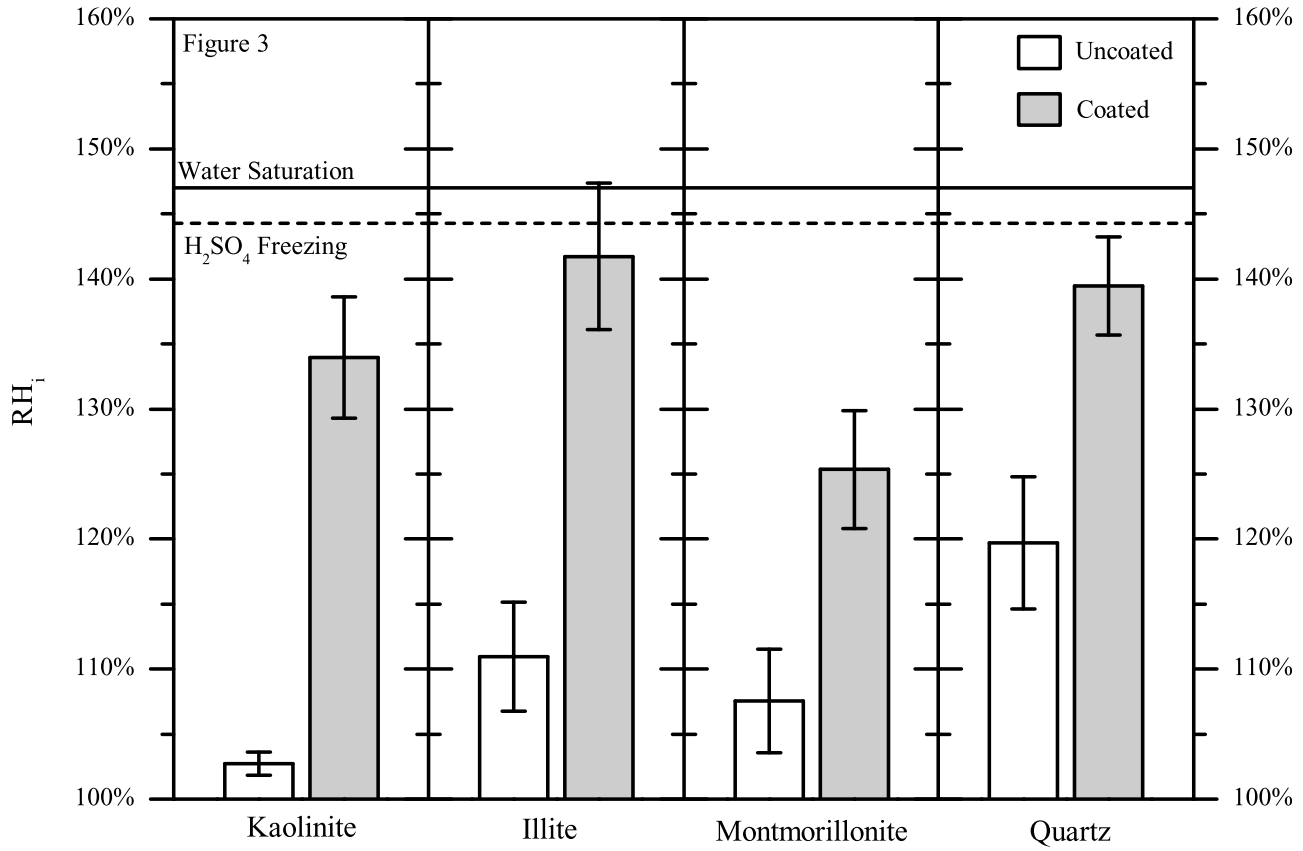


**Figure 3.** Average onset values for uncoated and sulfuric acid coated kaolinite, illite, montmorillonite and quartz particles studied using a frost point of 237 K. Error bars represent the 95% confidence intervals. The dashed line represents the threshold for homogeneous freezing of sulfuric acid droplets 8 $\mu$m in diameter at a freezing rate of 10 $s^{-1}$ [*Koop et al.*, 2000].

necessary for homogeneous freezing of the $H_2SO_4$ coating. As a result, heterogeneous freezing on these mineral cores is most likely still the dominant mechanism for nucleation in our experiments. For the case of illite, the average onset $RH_i$ overlaps with the conditions necessary for homogeneous nucleation of the $H_2SO_4$ coating if one considers the confidence intervals. This suggests that the coatings on illite may be "shutting off" heterogeneous freezing and favoring homogeneous nucleation of the aqueous coating.

[20] Recently, there have been several studies of the effect of sulfuric acid coatings on the ice nucleation properties of mineral dust particles. In a majority of the studies, a significant reduction in the ice nucleation efficiency after sulfuric acid coating was observed [*Archuleta et al.*, 2005; *Cziczo et al.*, 2009; *Gallavardin et al.*, 2008; *Möhler et al.*, 2008c]. Specifically, the coatings led to an increase in the $RH_i$ required for ice nucleation [*Archuleta et al.*, 2005; *Cziczo et al.*, 2009; *Gallavardin et al.*, 2008; *Möhler et al.*, 2008c], and the coated particles often required saturations approaching those for homogeneous freezing of aqueous solutions, as observed here [*Cziczo et al.*, 2009; *Möhler et al.*, 2008c]. However, in some cases, the impact of the coating was much less significant [*Archuleta et al.*, 2005; *Cziczo et al.*, 2009] or was not significant at all [*Knopf and Koop*, 2006], and for some minerals a decrease in $RH_i$ necessary for ice nucleation was observed [*Archuleta et al.*, 2005]. Differences in particle size, particle type, coating thickness, and temperature range studied may account for the variation between these results.

[21] Field measurements also support the hypothesis that atmospheric processing of mineral dust leads to a reduced ice nucleation ability. *Phillips et al.* [2008] compared field and laboratory data and concluded that atmospheric processing leads to a reduced ice nucleation efficiency. *Prenni et al.* [2009] noted the near absence of ice nuclei composed of mixed dust and sulfate, suggesting that coatings may affect the ability of these particles to act as ice nuclei. *DeMott et al.* [2003] noted that mineral dust particles that acted as good ice nuclei were relatively pure in form.

[22] The mechanism responsible for the deactivation of the ice nucleation ability of mineral dusts may be related to the mineral surface and how this surface interacts with the sulfuric acid coatings. Kaolinite, illite, and montmorillonite are clay minerals composed of layers of aluminosilicate sheets. The structure of quartz consists of silicon-oxygen tetrahedra linked by shared oxygen atoms [*Gualtieri*, 2000; *Viani et al.*, 2002].

[23] The composition of the sulfuric acid coating at the beginning of each experiment was very acidic; the starting pH of the coating was below zero. The point of zero charge (PZC) is defined as the pH at which the net surface charge is zero for a particular material [*Stumm*, 1992], and there is a PZC associated with the surfaces of each mineral dust studied. Kaolinite surfaces have PZCs at pH 6 or above,

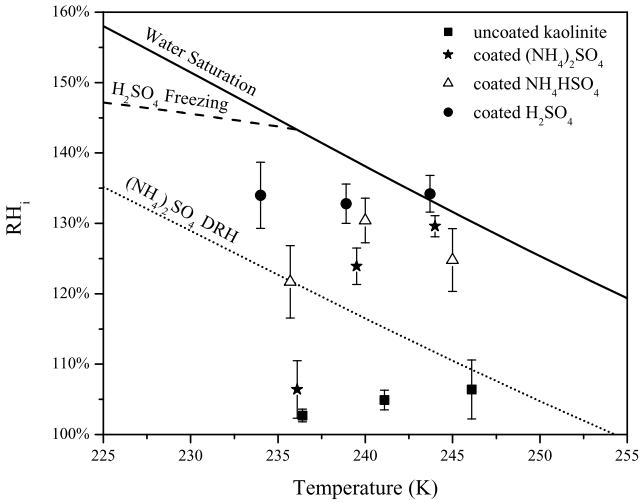


**Figure 4.** Onset results for $NH_4HSO_4$ coated kaolinite particles (open triangles). Included for comparison are previous results for uncoated kaolinite, $H_2SO_4$ coated and $(NH_4)_2SO_4$ coated kaolinite particles (filled symbols) [*Eastwood et al.*, 2009]. Error bars are given as 95% confidence intervals. Results shown are an average of at least six separate measurements. The dotted line represents the deliquescence relative humidity (DRH) for ammonium sulfate; the DRH line for $NH_4HSO_4$ lies below 70% $RH_i$ over the temperature range shown. The dashed line represents the threshold for homogeneous freezing of sulfuric acid droplets 8 $\mu$m in diameter at a freezing rate of 10 $s^{-1}$ [*Koop et al.*, 2000].

depending on the crystalline face [*Stumm*, 1992]; the surfaces of illite and montmorillonite have PZCs at 2.2 or higher [*Kriaa et al.*, 2009; *Parks*, 1965; *Rozalen et al.*, 2009]; and quartz has a PZC of 2.2 [*Parks*, 1965]. Accordingly, the exposed areas of the mineral particles would be protonated under the acidic conditions in our experiments. The positively charged, protonated environment should facilitate strong adsorption of sulfate anions to the mineral surface, changing the chemical and physical properties of the surfaces [*Eastwood et al.*, 2009]. It is therefore hypothesized that the ice nucleation properties of the mineral dusts would change when coated with sulfuric acid. Molecular simulations similar to recent simulations on uncoated mineral surfaces would be useful to better understand these processes [*Croteau et al.*, 2008; *Hu and Michaelides*, 2007; 2008].

### 3.2. Effect of Ammonium-to-Sulfate Ratio on the Ice Nucleation Properties of Kaolinite

[24] Shown in Figure 4 are the results for kaolinite coated with ammonium bisulfate. Also included for comparison are the results for uncoated, sulfuric acid coated, and ammonium sulfate coated kaolinite particles. Each data point in this figure is the average from at least six separate measurements done for each particle type and temperature. The error bars represent 95% confidence intervals of the onset $RH_i$ values.

[25] From Figure 4 one can conclude that kaolinite particles coated with ammonium bisulfate are less efficient ice nuclei than uncoated kaolinite particles; the coating increased the onset $RH_i$ by approximately 18 to 26% compared to uncoated kaolinite particles. Also, in general, it appears that sulfuric acid coatings (ASR = 0) have the largest effect on the nucleation properties of kaolinite. This is most clear at the lowest temperatures studied. Ammonium bisulfate coatings (ASR = 1) appear to be intermediate between sulfuric acid and ammonium sulfate. Again, these differences are clearest at the lowest temperatures.

[26] As suggested above, the sulfuric acid coating may hinder ice nucleation by protonation of the kaolinite surface and by adsorption of sulfate anions to the protonated surface. The pH of the ammonium bisulfate coating at the beginning of each experiment was 0.87. Hence, a similar effect can occur for ammonium bisulfate, which would explain why ammonium bisulfate also changes significantly the ice nucleation properties of kaolinite particles. It is also possible that the acid solutions irreversibly react with the mineral surfaces. For example, recently it was shown that when mineral surfaces are exposed to pH values <1.0, an increase in dissolution of aluminosilicates with decreasing pH was observed as well as precipitation of an amorphous silica phase [*Shaw et al.*, 2009]. These processes could be occurring in our experiments (and in the atmosphere) and potentially could explain the difference between the sulfuric acid and ammonium bisulfate coatings, since the sulfuric acid solutions have lower pH values and lead to increased dissolution rates.

[27] Figure 4 also shows that ammonium sulfate coatings (ASR = 2) are most sensitive to temperature. This is most likely related to the phase of the coatings. $H_2SO_4$ does not undergo deliquescence and effluorescence and $NH_4HSO_4$ deliquescences at <70% $RH_i$ over the temperature range studied here. As a result, $H_2SO_4$ and $NH_4HSO_4$ coatings remained liquid during our experiments. In contrast, $(NH_4)_2SO_4$ coatings can remain solid for some of the conditions used in our experiments. The deliquescence relative humidity for $(NH_4)_2SO_4$ is shown in Figure 4 as a dotted line. If the $(NH_4)_2SO_4$ coatings are crystalline, this solid can also act as a heterogeneous ice nuclei (at least for bigger particles) [*Abbatt et al.*, 2006; *Baustian et al.*, 2010; *Shilling et al.*, 2006; *Zuberi et al.*, 2002]. For a further discussion of the $(NH_4)_2SO_4$ results as well as an explanation of the temperature trend observed for $(NH_4)_2SO_4$ coatings, see *Eastwood et al.* [2009].

### 3.3. Ice Nucleation on Uncoated SNOMAX

[28] The onset results for uncoated and sulfuric acid coated SNOMAX particles are presented as a function of surface area in Figure 5. Each data point represents one freezing event, and the error bars represent the uncertainty in $RH_i$. The onset data for SNOMAX have been summarized as a function of temperature in Figure 6.

[29] The results for sulfuric acid coated SNOMAX are discussed in this next section. The results for the uncoated case, shown in Figures 5 and 6, show that ice nucleation occurs at ~110–120% $RH_i$, independent of temperature. This indicates that SNOMAX is a reasonably good ice nucleus at atmospherically relevant conditions.

[30] The ice nucleation properties of SNOMAX have been investigated in other studies [*Möhler et al.*, 2008b; *Ward and DeMott*, 1989; *Wood et al.*, 2002], but these measurements were done at 258 K and above. To our knowledge, our studies are the first to look at freezing of these particles at lower temperatures. There have also been numerous studies

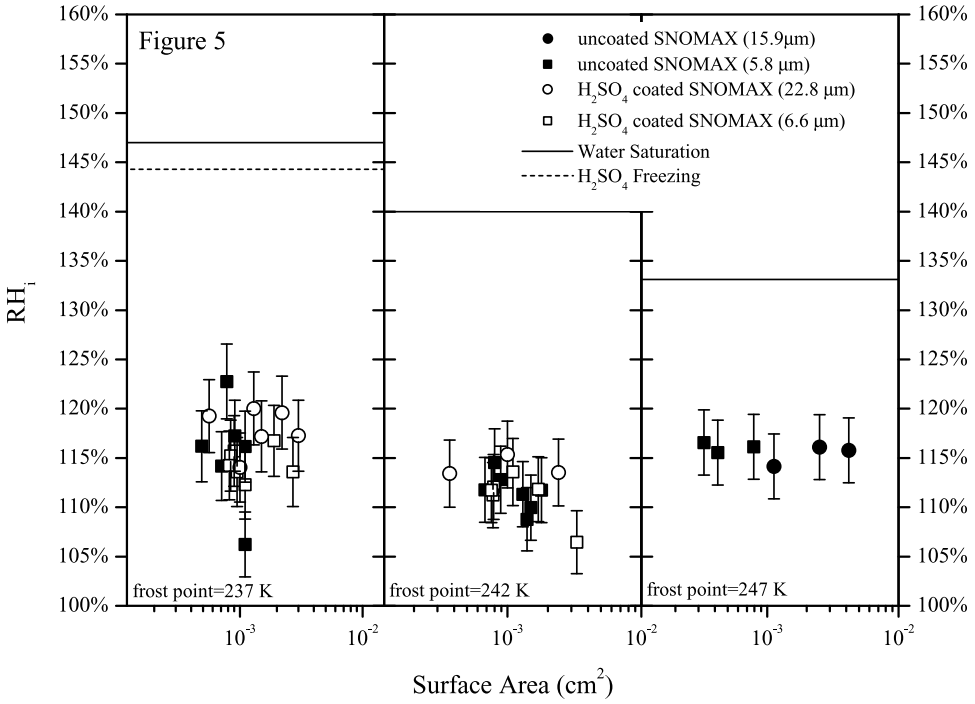


**Figure 5.** Ice nucleation measurements on uncoated (closed symbols) and $H_2SO_4$ coated (open symbols) SNOMAX particles. Data are plotted as onset $RH_i$ against surface area ($cm^2$). Squares and circles represent particles made using a commercially available and in-house built nebulizer, respectively. The dashed line in the left image represents the threshold for homogeneous freezing of sulfuric acid droplets 8 $\mu$m in diameter at a freezing rate of 10 $s^{-1}$ [*Koop et al.*, 2000]; this line lies above water saturation for the middle and right images.

on the ice nucleation properties of unaltered *P. syringae*. These studies have also focused on warmer temperatures than employed in the current study, so the results are not directly comparable [*Lindow et al.*, 1978; 1989; *Möhler et al.*, 2008b; *Vali*, 1971; *Wolber et al.*, 1986].

### 3.4. Effect of Sulfuric Acid Coatings on the Ice Nucleation Properties of SNOMAX

[31] The ice nucleation results for uncoated and sulfuric acid coated SNOMAX particles are compared in Figures 5 and 6. Unlike the mineral dust results, the sulfuric acid coatings did not hinder the ice-nucleating ability of SNOMAX particles.

[32] The fact that the uncoated and coated results were similar was somewhat surprising in light of the mineral dust results presented earlier in this paper. We offer here a few different explanations. First, it is possible that a few SNOMAX particles were not completely covered with the acid solution, providing sites for ice nucleation. This did not occur in the mineral dust studies, which had identical experimental conditions. Nevertheless, it may have occurred in the SNOMAX studies. Unfortunately, it is not possible to verify that every particle is completely covered in our experiments. Even if some SNOMAX particles were not covered completely, these particles were still exposed to a dilute acid solution ($2 \times 10^{-2}$ M $H_2SO_4$, pH 1.6) for 2–4 days prior to nebulization. At a minimum, our results show that long exposure to dilute acid solutions does not modify the ice nucleation properties of SNOMAX particles at the temperatures and relative humidities studied.

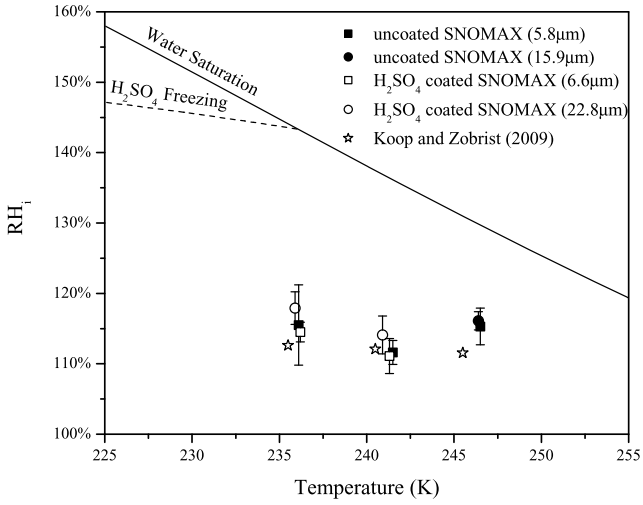


**Figure 6.** Onset results for uncoated (filled symbols) and $H_2SO_4$ coated (open symbols) SNOMAX. Open stars represent freezing of aqueous acid solution drops containing SNOMAX inclusions from *Koop and Zobrist* [2009]. Error bars represent the 95% confidence intervals. Results shown are an average of at least three separate measurements. Squares and circles represent particles made using a commercially available and in-house built nebulizer, respectively. The dashed line represents the threshold for homogeneous freezing of sulfuric acid droplets 8 $\mu$m in diameter at a freezing rate of 10 $s^{-1}$ [*Koop et al.*, 2000].

**Table 3.** $J_{het}$ Values and Contact Angles for Uncoated and Sulfuric Acid Coated Mineral Dusts and Uncoated SNOMAX

| Mineral | Type | Onset Temperature (K) | $RH_i$ (%) | $J_{het}$ ($cm^{-2}$ $s^{-1}$) | $J_{het,\ upper}$ ($cm^{-2}$ $s^{-1}$) | $J_{het,\ lower}$ ($cm^{-2}$ $s^{-1}$) | $\theta_{lower}$ | $\theta$ | $\theta_{upper}$ |
|---|---|---|---|---|---|---|---|---|---|
| Kaolinite | Pure | 236 | 104 ± 2 | 281 | 2814 | 3 | 3 | 9 | 14 |
| Kaolinite | Coated | 234 | 134 ± 5 | 224 | 2237 | 2 | 58 | 72 | 100 |
| Illite | Pure | 237 | 112 ± 5 | 1292 | 12921 | 13 | 11 | 15 | 18 |
| Illite | Coated | 235 | 142 ± 6 | 1000 | 10000 | 10 | 64 | 79 | 109 |
| Montmorillonite | Pure | 236 | 108 ± 4 | 931 | 9307 | 9 | 8 | 12 | 16 |
| Montmorillonite | Coated | 235 | 125 ± 5 | 1281 | 12808 | 13 | 48 | 60 | 80 |
| Quartz | Pure | 236 | 120 ± 5 | 606 | 6057 | 6 | 17 | 20 | 23 |
| Quartz | Coated | 235 | 140 ± 4 | 805 | 8046 | 8 | 63 | 78 | 108 |
| SNOMAX | Pure | 236 | 116 ± 6 | 127 | 1271 | 1 | 15 | 18 | 21 |
| SNOMAX | Pure | 242 | 112 ± 2 | 94 | 936 | 1 | 13 | 16 | 19 |
| SNOMAX | Pure | 246 | 116 ± 1 | 137 | 1370 | 1 | 16 | 19 | 22 |

[33] Another possible explanation for the coated SNOMAX results is that the acid solution does not significantly modify active ice nucleation sites present on SNOMAX. It is thought that the reason SNOMAX and unaltered *P. syringae* are good IN is due to a certain protein located in the outer cell membrane. Experimental evidence has shown that the protein forms aggregates on the outer membrane in such a manner that the hydrophilic repetitive region of the protein provides a lattice match for the hydrogen bonding requirements of ice [*Green and Warren*, 1985; *Gurian-Sherman and Lindow*, 1993; *Lee et al.*, 1995; *Morris et al.*, 2004; *Szyrmer and Zawadzki*, 1997]. Our current results may suggest that sulfuric acid solutions do not modify this environment significantly enough to influence ice nucleation for the temperatures and $RH_i$ values explored.

[34] Recently, the freezing properties of dilute and concentrated acid solution droplets containing SNOMAX were studied using differential scanning calorimetry [*Koop and Zobrist*, 2009]. Koop and Zobrist reported results in terms of freezing temperatures and water activities. Shown in Figure 6 are the freezing conditions predicted by the *Koop and Zobrist* [2009] data for the temperatures used in our experiments. These predictions are in good agreement with the results we obtained for coated particles. This agreement provides some support for the finding that the particles in our experiments were completely coated and also that coatings by acids have relatively little effect on the freezing conditions, at least for the temperature range we studied.

[35] Several studies also investigated the freezing properties of dilute acid solutions containing other species of bacteria, many in the *Pseudomonas* genera, known to be effective IN. These studies were done at warm temperatures and as a result are not directly comparable to our studies. Nevertheless, it is interesting to note that in the experiments where an acid effect was observed, the freezing temperature, even in the acid solutions, was still above −11 °C; which is above the temperature range employed in our studies [*Chen et al.*, 2002; *Kawahara et al.*, 1996; *Obata et al.*, 1993; *Pouleur et al.*, 1992; *Yin et al.*, 2005]. Also, one study noted that the freezing temperature of one species of *Pseudomonas* was not sensitive to the pH range studied (3.5 to 5.0) [*Kawahara et al.*, 1995].

### 3.5. Nucleation rate, $J_{het}$

[36] The heterogeneous nucleation rate, $J_{het}$, is defined as the number of nucleation events per unit surface area of solid material per unit time. Note that $J_{het}$ is referred to as both a rate [*Pruppacher and Klett*, 1997; *Hung et al.*, 2003; *Archuleta et al.*, 2005] and a rate coefficient [*Dymarska et al.*, 2006; *Marcolli et al.*, 2007] in the literature. The heterogeneous nucleation rate is related to the onset data through equation (1):

$$J_{het} = \frac{\omega}{A_s t}, \tag{1}$$

where $\omega$ is the number of ice crystals nucleated, $A_s$ is the total mineral dust/SNOMAX surface area available for heterogeneous nucleation, and $t$ is the observation time. At the onset of ice nucleation, $\omega$ was equal to 1.

[37] Table 3 lists the nucleation rates determined in our experiments. The uncertainty in $J_{het}$ was determined by considering the uncertainties in $A_s$ and $t$. We used 10 s for the observation time with an upper limit of 20 s (the time between image captures) and a lower limit of 1 s. Note, however, that nucleation may have happened at a shorter time than 1 s. If this is the case, the calculated nucleation rates are lower limits to the true nucleation rates. For the surface area, we used the geometric surface area of the particles determined directly from the optical microscope. For an upper limit to the surface area, we multiplied the geometric surface area of the particles by a factor of 50 on the basis of scanning electron microscope measurements of kaolinite particles [*Eastwood et al.*, 2008]. The data shown in Table 3 suggest that our experiments are typically sensitive to values of $J_{het}$ ranging from 2 to 13,000 $cm^{-2}$ $s^{-1}$.

### 3.6. Classical Nucleation Theory Parameters From $J_{het}$

[38] The applicability of standard classical nucleation theory to heterogeneous nucleation on minerals and biological particles remains to be determined. In fact, some measurements show that, for precise predictions, active site theory is required [*Archuleta et al.*, 2005; *Hung et al.*, 2003; *Marcolli et al.*, 2007]. Nevertheless, classical nucleation theory is a relatively convenient and simple way to parameterize laboratory data. Hence, classical nucleation theory is a reasonable starting point for analyzing our experimental data. Below in this section, we analyze the nucleation rates using classical nucleation theory. From this analysis, we determined the contact angle between an ice embryo and the mineral surface.

[39] In this analysis, we focus on the results for uncoated minerals, uncoated SNOMAX, and sulfuric acid coated minerals studied at an ice frost point of 237 K. We did not

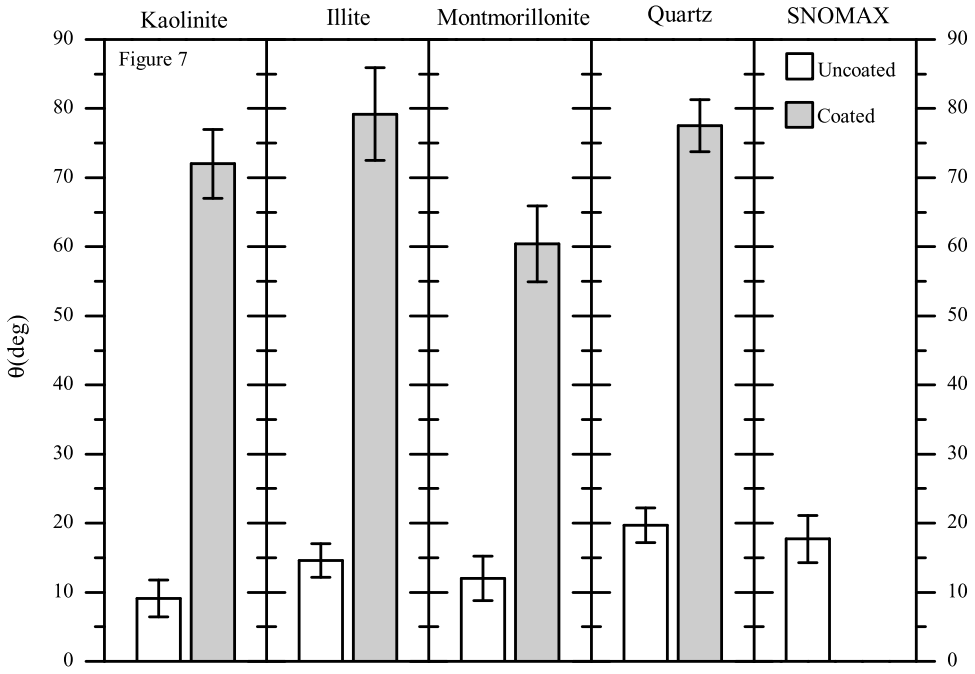


**Figure 7.** Average contact angles for uncoated and sulfuric acid coated mineral dust particles and uncoated SNOMAX particles studied at a frost point of 237 K. Error bars are given as 95% confidence intervals. The sulfuric acid coated SNOMAX results were excluded because the coated results were not statistically different from the uncoated results.

do a similar analysis for the ammonium bisulfate coated studies because the theromodynamic parameters of the ammonium bisulfate solution needed for the calculations are not readily available. Also, we excluded the sulfuric acid coated SNOMAX results because the coated results were not statistically different from the uncoated results.

[40] All the uncoated results that we focused on for the classical nucleation theory analysis corresponds to deposition freezing. To convert the nucleation rates for these deposition freezing results to contact angles, we used the procedure outlined in our previous paper [*Eastwood et al.*, 2008]. For details on the calculations, please see this previous publication.

[41] All the sulfuric acid coated results that were analyzed using classical nucleation theory correspond to immersion freezing. According to standard classical nucleation theory, the rate of heterogeneous nucleation ($J_{het}$) by immersion freezing is defined as follows [*Archuleta et al.*, 2005; *Pruppacher*, 1997; *Tabazadeh et al.*, 1997; 2000]:

$$J_{het,imm} = A \exp\left(\frac{-\Delta F_{g,het} - \Delta g}{kT}\right), \tag{2}$$

where $A$ is the preexponential factor in units of cm$^{-2}$ s$^{-1}$, $\Delta F_{g,het}$ is the free energy of formation of the critical embryo on the surface in units of $J$, $k$ is the Boltzmann constant in $J$ K$^{-1}$, $T$ is the onset temperature in K, and $\Delta g$ is the activation energy for the diffusion of a water molecule across the ice-water interface in units of $J$.

[42] The critical embryo is approximated as a spherical cap on a curved surface. The free energy of formation of the critical embryo for immersion freezing can be described by the following equation [*Pruppacher*, 1997]:

$$\Delta F_{g,het} = \frac{4}{3}\pi r_g^2 \sigma_{i/s} f(m,x), \tag{3}$$

where $r_g$ is the radius of the ice embryo; $\sigma_{i/s}$ is the surface tension at the ice-sulfuric acid solution interface, $f(m,x)$ is the geometric factor, $m$ is the compatibility parameter for ice on a solid substrate, and $x$ is the ratio of the radius of the substrate to the radius of spherical ice germ. Assuming the radius of the substrate to be much larger than the radius of the ice germ (a good approximation under our experimental conditions), $f(m,x)$ is defined as follows:

$$f(m,x) = \frac{m^3 - 3m + 2}{4}. \tag{4}$$

The compatibility parameter, $m$, is equal to cos$\theta$, where $\theta$ is the contact angle between an ice nucleus and the solid surface.

[43] Also, the radius of the ice embryo is given (in cm) as follows [*Archuleta et al.*, 2005; *DeMott and Lynch*, 2002; *Khvorostyanov and Sassen*, 1998]:

$$r_g = \frac{2\sigma_{i/s}}{\rho_i L_{ef}\left[\ln\left(\frac{T_0}{T}\right) a_w^G\right]}, \tag{5}$$

where $\rho_i$ (g cm$^{-3}$) is the temperature-dependent density of ice, $\sigma_{i/s}$ (erg cm$^{-2}$) is as defined above, $L_{ef}$ (cal g$^{-1}$) is the effective latent heat of formation, $T_0$ is the triple point of water, $a_w$ is the water activity, and $G$ is a dimensionless parameter equal to $RT/L_{ef}M_w$ [*Khvorostyanov and Sassen*, 1998], where $M_w$ is the molecular weight of water.

[44] We calculated $\theta$ according to the method used by *Archuleta et al.*, [2005]. First, equation (2) was used to obtain $\Delta F_{g,het}$ using the temperature-dependent expression for $\Delta g$ (ergs $\times$ $10^{13}$) from *Tabazadeh et al.*, [1997], the experimentally determined $J_{het,imm}$ values from equation (1), and a preexponential factor, $A$, equal to $10^{20}$ cm$^{-2}$ s$^{-1}$ [*Fletcher*, 1969; *Hung et al.*, 2003]. Second, equation (5) was used to find $r_g$. In this calculation, we used $\rho_i$ from *Pruppacher*, [1997], $\sigma_{i/s}$ from *Tabazadeh et al.*, [2000], and $L_{ef}$ from *Khvorostyanov and Sassen*, [1998]. Third, equation (3) was used to find $f(m,x)$. Fourth, equation (4) can be evaluated for $m$, and finally, the compatibility parameter can be used to find the contact angle, $\theta$.

[45] In Table 3, the nucleation rates and contact angles calculated using the procedures discussed above are listed for uncoated and sulfuric acid coated mineral dust particles, as well as the uncoated SNOMAX results. The upper and lower limits for $J_{het}$ (and hence $\theta$) were determined using the upper and lower limits to the observation times in our experiments and the upper limits to the surface area estimated from scanning electron microscopy (see section 3.5 for more details). The contact angle values for measurements done at an ice frost point of 237 K are also illustrated in Figure 7. The data show that for uncoated ice nuclei, the contact angles are small (below ~20°). For mineral dust particles coated with sulfuric acid, the contact angles are larger (above ~60°). These values may be useful for future modeling studies of ice nucleation in the atmosphere and for comparing results between different laboratories. However, keep in mind that our calculations assume one contact angle for a given sample type. In reality, particles within a given sample type may have a range of ice nucleation efficiencies and hence a range of contact angles [*Archuleta et al.*, 2005; *Hung et al.*, 2003; *Marcolli et al.*, 2007]. If this is the case, contact angles determined from onset conditions (as done in the current study) may overestimate the nucleation rate on the same sample exposed to longer nucleation times or $RH_i$ values above the onset values. For these reasons, extrapolation outside our experimental conditions should be done with caution. This will be addressed in more detail in a future publication [*Wheeler et al.*, unpublished manuscript, 2010].

## 4. Conclusions

[46] An optical microscope coupled to a flow cell was used to study the heterogeneous ice nucleation properties of uncoated and coated mineral dust and SNOMAX particles at temperatures ranging from 234 to 247 K. The results show that $H_2SO_4$ coatings significantly modified the heterogeneous ice nucleation properties of all the minerals studied. For kaolinite and illite, the acid coatings increased the onset $RH_i$ by ~30%; for montmorillonite and quartz, the acid coatings increased the onset $RH_i$ by ~20%. Our studies also show that $NH_4HSO_4$ coatings influence the heterogeneous ice nucleation properties of kaolinite particles. The coated particles are less effective at nucleating ice than uncoated particles, with the onset $RH_i$ increasing by approximately 18 to 26%, depending on temperature.

[47] Onset results indicate that uncoated SNOMAX, a biological IN made from cells of *P. syringae*, is a reasonably good ice nucleus, having onset values between 110 and 120% $RH_i$. Unlike the mineral dust results, the sulfuric acid coatings did not hinder the heterogeneous ice-nucleating ability of SNOMAX particles within experimental uncertainty. One possible explanation is that a few SNOMAX particles were not completely covered with the acid solution, providing a bare site for ice nucleation. However, the agreement between our coated results and the recent results by *Koop and Zobrist* [2009] for sulfuric acid solutions containing SNOMAX provides some support for the finding that the particles in our experiments are completely coated. Another possible explanation for the coated SNOMAX results is that the acid solution does not significantly modify the active ice nucleation sites for SNOMAX, which are thought to be certain proteins located in the outer cell membrane.

[48] The heterogeneous nucleation rates ($J_{het}$) and contact angles ($\theta$) were determined according to classical nucleation theory for all uncoated and sulfuric acid coated mineral dusts studied and for uncoated SNOMAX particles. The data show that for all uncoated ice nuclei, the contact angles are small (below ~20°). For mineral dust particles coated with sulfuric acid, the contact angles are larger (above ~60°). The contact angles presented here are average values; however, previous work has indicated that it is the probability distribution function (PDF) of contact angles that is important to measure in future work [*Eidhammer et al.*, 2009; *Marcolli et al.*, 2007; *Phillips et al.*, 2008]. *Marcolli et al.* [2007] showed that the most active ice nucleation sites are rare in that they lie at the tail of the PDF, and furthermore, that it is these sites that are involved in ice nucleation in a population of particles of a given type.

[49] Combined, our results support the idea that anthropogenic emissions of $SO_2$ and $NH_3$ may influence the heterogeneous ice-nucleating properties of mineral dust particles by increasing the relative humidity required for ice nucleation.

[50] **Acknowledgments.** We thank P. J. DeMott for helpful discussions on the immersion mode calculations. This research was supported by the Canadian Foundation for Climate and Atmospheric Sciences (CFCAS), the National Sciences and Engineering Research Council of Canada (NSERC), and the Canada Research Chairs program.

## References

Abbatt, J. P. D., S. Benz, D. J. Cziczo, Z. Kanji, U. Lohmann, and O. Möhler (2006), Solid ammonium sulfate aerosols as ice nuclei: A pathway for cirrus cloud formation, *Science*, *313*(5794), 1770–1773, doi:10.1126/science.1129726.

Archuleta, C. M., P. J. DeMott, and S. M. Kreidenweis (2005), Ice nucleation by surrogates for atmospheric mineral dust and mineral dust/sulfate particles at cirrus temperatures, *Atmos. Chem. Phys.*, *5*, 2617–2634.

Ariya, P. A., J. Sun, N. A. Eltouny, E. D. Hudson, C. T. Hayes, and G. Kos (2009), Physical and chemical characterization of bioaerosols: Implications for nucleation processes, *Int. Rev. Phys. Chem.*, *28*(1), 1–32, doi:10.1080/01442350802597438.

Baker, M. B., and T. Peter (2008), Small-scale cloud processes and climate, *Nature*, *451*(7176), 299–300, doi:10.1038/nature06594.

Baustian, K. J., M. E. Wise, and M. A. Tolbert (2010), Depositional ice nucleation on solid ammonium sulfate and glutaric acid particles, *Atmos. Chem. Phys.*, *10*, 2307–2317.

Cantrell, W., and A. Heymsfield (2005), Production of ice in tropospheric clouds: A review, *Bull. Am. Meteorol. Soc.*, *86*(6), 795–807, doi:10.1175/BAMS-86-6-795.

Chen, M. L., T. K. Chiou, and S. T. Jiang (2002), Isolation of ice-nucleating active bacterium from mackerel and its properties, *Fish. Sci. (Tokyo)*, *68*(4), 934–941, doi:10.1046/j.1444–2906.2002.00513.x.

Chester, R., J. J. Griffin, H. Elderfie, L. R. Johnson, and R. C. Padgham (1972), Eolian dust along eastern margins of Atlantic Ocean, *Mar. Geol.*, *13*(2), 91–105, doi:10.1016/0025-3227(72)90048-5.

Christner, B. C., R. Cai, C. E. Morris, K. S. McCarter, C. M. Foreman, M. L. Skidmore, S. N. Montross, and D. C. Sands (2008a), Geographic, seasonal, and precipitation chemistry influence on the abundance and activity of biological ice nucleators in rain and snow, *Proc. Natl. Acad. Sci. USA*, *105*(48), 18,854–18,859, doi:10.1073/pnas.0809816105.

Christner, B. C., C. E. Morris, C. M. Foreman, R. M. Cai, and D. C. Sands (2008b), Ubiquity of biological ice nucleators in snowfall, *Science*, *319*(5867), 1214–1214, doi:10.1126/science.1149757.

Clegg, S. L., P. Brimblecombe, and A. S. Wexler (1998), Thermodynamic model of the system $H^+$-$NH_4^+$-$SO_4^{2-}$-$NO_3^-$-$H_2O$ at tropospheric temperatures, *J. Phys. Chem. A*, *102*(12), 2137–2154, doi:10.1021/jp973042r.

Croteau, T., A. K. Bertram, and G. N. Patey (2008), Adsorption and structure of water on Kaolinite surfaces: Possible insight into ice nucleation from grand canonical Monte Carlo calculations, *J. Phys. Chem. A*, *112*(43), 10,708–10,712, doi:10.1021/jp805615q.

Cziczo, D. J., K. D. Froyd, S. J. Gallavardin, O. Moehler, S. Benz, H. Saathoff, and D. M. Murphy (2009), Deactivation of ice nuclei due to atmospherically relevant surface coatings, *Environ. Res. Lett.*, *4*(4), 044013, doi:10.1088/1748-9326/4/4/044013.

Cziczo, D. J., D. M. Murphy, P. K. Hudson, and D. S. Thomson (2004), Single particle measurements of the chemical composition of cirrus ice residue during CRYSTAL-FACE, *J. Geophys. Res.*, *109*, D04201, doi:10.1029/2003JD004032.

DeMott, P. J., D. J. Cziczo, A. J. Prenni, D. M. Murphy, S. M. Kreidenweis, D. S. Thomson, R. Borys, and D. C. Rogers (2003), Measurements of the concentration and composition of nuclei for cirrus formation, *Proc. Natl. Acad. Sci. USA*, *100*(25), 14655–14660, doi:10.1073/pnas.2532677100.

DeMott, P. J., and D. K. Lynch (Eds.) (2002), *Laboratory Studies of Cirrus Cloud Processes*, *Cirrus*, pp. 102–136, Oxford University Press, New York.

Dymarska, M., B. J. Murray, L. M. Sun, M. L. Eastwood, D. A. Knopf, and A. K. Bertram (2006), Deposition ice nucleation on soot at temperatures relevant for the lower troposphere, *J. Geophys. Res.*, *111*, D04204, doi:10.1029/2005JD006627.

Eastwood, M. L., S. Cremel, C. Gehrke, E. Girard, and A. K. Bertram (2008), Ice nucleation on mineral dust particles: Onset conditions, nucleation rates and contact angles, *J. Geophys. Res.*, *113*, D22203, doi:10.1029/2008JD010639.

Eastwood, M. L., S. Cremel, M. Wheeler, B. J. Murray, E. Girard, and A. K. Bertram (2009), Effects of sulfuric acid and ammonium sulfate coatings on the ice nucleation properties of kaolinite particles, *Geophys. Res. Lett.*, *36*, L02811, doi:10.1029/2008GL035997.

Eidhammer, T., P. J. DeMott, and S. M. Kreidenweis (2009), A comparison of heterogeneous ice nucleation parameterizations using a parcel model framework, *J. Geophys. Res.*, *114*, D06202, doi:10.1029/2008JD011095.

Ettner, M., S. K. Mitra, and S. Borrmann (2004), Heterogeneous freezing of single sulfuric acid solution droplets: laboratory experiments utilizing an acoustic levitator, *Atmos. Chem. Phys.*, *4*, 1925–1932.

Fletcher, N. H. (1969), Active sites and ice crystal nucleation, *J. Atmos. Sci.*, *26*(6), 1266–1271, doi:10.1175/1520-0469(1969)026<1266:ASAICN>2.0.CO;2.

Gallavardin, S. J., K. D. Froyd, U. Lohmann, O. Moehler, D. M. Murphy, and D. J. Cziczo (2008), Single particle laser mass spectrometry applied to differential ice nucleation experiments at the AIDA chamber, *Aerosol Sci. Technol.*, *42*(9), 773–791, doi:10.1080/02786820802339538.

Glaccum, R. A., and J. M. Prospero (1980), Saharan aerosols over the tropical North-Atlantic–mineralogy, *Mar. Geol.*, *37*(3–4), 295–321, doi:10.1016/0025-3227(80)90107-3.

Green, R. L., and G. J. Warren (1985), Physical and functional repetition in a bacterial ice nucleation gene, *Nature*, *317*(6038), 645–648, doi:10.1038/317645a0.

Gross, D. C., Y. S. Cody, E. L. Proebsting, G. K. Radamaker, and R. A. Spotts (1983), Distribution, population-dynamics, and characteristics of ice nucleation-active bacteria in deciduous fruit tree orchards, *Appl. Environ. Microbiol.*, *46*, 1370–1379.

Gualtieri, A. F. (2000), Accuracy of XRPD QPA using the combined Rietveld-RIR method, *J. Appl. Crystallogr.*, *33*(2), 267–278, doi:10.1107/S002188989901643X.

Gurian-Sherman, D., and S. E. Lindow (1993), Bacterial ice nucleation: Significance and molecular basis, *FASEB J.*, *7*, 1338–1343.

Hegg, D. A., and M. B. Baker (2009), Nucleation in the atmosphere, *Rep. Prog. Phys.*, *72*(5), 056801, doi:10.1088/0034-4885/72/5/056801.

Heintzenberg, J., K. Okada, and J. Strom (1996), On the composition of non-volatile material in upper tropospheric aerosols and cirrus crystals, *Atmos. Res.*, *41*(1), 81–88, doi:10.1016/0169-8095(95)00042-9.

Hinz, K. P., A. Trimborn, E. Weingartner, S. Henning, U. Baltensperger, and B. Spengler (2005), Aerosol single particle composition at the Jungfraujoch, *J. Aerosol Sci.*, *36*(1), 123–145, doi:10.1016/j.jaerosci.2004.08.001.

Hirano, S. S., L. S. Baker, and C. D. Upper (1985), Ice nucleation temperature of individual leaves in relation to population sizes of ice nucleation active bacteria and frost injury, *Plant Physiol.*, *77*, 259–265.

Houghton, J. T., Y. Ding, D. J. Griggs, M. Noguer, P. J. van der Linden, X. Dai, K. Maskell, and C. A. Johnson (Eds.) (2001), *IPCC, 2001: Climate Change 2001: The Scientific Basis. Contribution of Working Group I to the Third Assessment Report of the Intergovernmental Panel on Climate Change*, 881 pp., Cambridge University Press, Cambridge, U. K., and New York.

Hu, X. L., and A. Michaelides (2007), Ice formation on kaolinite: Lattice match or amphoterism?, *Surf. Sci.*, *601*(23), 5378–5381, doi:10.1016/j.susc.2007.09.012.

Hu, X. L., and A. Michaelides (2008), Water on the hydroxylated (001) surface of kaolinite: From monomer adsorption to a flat 2D wetting layer, *Surf. Sci.*, *602*(4), 960–974, doi:10.1016/j.susc.2007.12.032.

Hung, H. M., A. Malinowski, and S. T. Martin (2003), Kinetics of heterogeneous ice nucleation on the surfaces of mineral dust cores inserted into aqueous ammonium sulfate particles, *J. Phys. Chem. A*, *107*(9), 1296–1306, doi:10.1021/jp021593y.

Kanji, Z. A., O. Florea, and J. P. D. Abbatt (2008), Ice formation via deposition nucleation on mineral dust and organics: Dependence of onset relative humidity on total particulate surface area, *Environ. Res. Lett.*, *3*, 025004, doi:10.1088/1748-9326/3/2/025004.

Kawahara, H., Y. Tanaka, and H. Obata (1995), Isolation and characterization of a novel ice-nucleating bacterium, *Pseudomonas*, which has stable activity in acidic solution, *Biosci., Biotechnol., Biochem.*, *59*, 1528–1532.

Kawahara, H., H. Ikugawa, and H. Obata (1996), Isolation and characterization of a marine ice-nucleating bacterium, *Pseudomonas* sp KUIN-5, which produces cellulose and secretes it in the culture broth, *Biosci., Biotechnol., Biochem.*, *60*, 1474–1478.

Khvorostyanov, V., and K. Sassen (1998), Toward the theory of homogeneous nucleation and its parameterization for cloud models, *Geophys. Res. Lett.*, *25*, 3155–3158.

Knopf, D. A., and T. Koop (2006), Heterogeneous nucleation of ice on surrogates of mineral dust, *J. Geophys. Res.*, *111*, D12201, doi:10.1029/2005JD006894.

Koop, T., B. P. Luo, A. Tsias, and T. Peter (2000), Water activity as the determinant for homogeneous ice nucleation in aqueous solutions, *Nature*, *406*(6796), 611–614, doi:10.1038/35020537.

Koop, T., and B. Zobrist (2009), Parameterizations for ice nucleation in biological and atmospheric systems, *Phys. Chem. Chem. Phys.*, *11*(46), 10839–10850, doi:10.1039/b914289d.

Kriaa, A., N. Hamdi, and E. Srasra (2009), Proton adsorption and acid-base properties of Tunisian illites in aqueous solution, *J. Struct. Chem.*, *50*(2), 273–287, doi:10.1007/s10947–009-0039–6.

Lammel, G., T. Engelhardt, A. Leip, C. Neususs, A. Rohrl, B. Wehner, A. Wiedensohler, and P. Wieser (2005), Transformation of aerosol chemical properties due to transport over a city, *J. Atmos. Chem.*, *51*(1), 95–117, doi:10.1007/s10874-005-7646-1.

Lee, R. E. L., G. L. Warren, and L. V. Gusta (1995), *Biological Ice Nucleation and Its Applications*, APS Press, St. Paul, MN.

Lindow, S. E., D. C. Arny, and C. D. Upper (1978), *Erwinia herbicola*: Bacterial ice nucleus active in increasing frost injury to corn, *Phytopathology*, 68(3), 523–527, doi:10.1094/Phyto-68–523.

Lindow, S. E., E. Lahue, A. G. Govindarajan, N. J. Panopoulos, and D. Gies (1989), Localization of ice nucleation activity and the ICEC gene-product in *Pseudomonas-syringae* and *Escherichia-coli*, *Mol. Plant-Microbe Interact.*, 2(5), 262–272, doi:10.1094/MPMI-2–262.

Marcolli, C., S. Gedamke, T. Peter, and B. Zobrist (2007), Efficiency of immersion mode ice nucleation on surrogates of mineral dust, *Atmos. Chem. Phys.*, *7*(19), 5081–5091, doi:10.1007/978-1-4020-6475-3_5.

McNaughton, C. S., et al. (2009), Observations of heterogeneous reactions between Asian pollution and mineral dust over the eastern North Pacific during INTEX-B, *Atmos. Chem. Phys.*, *9*, 8283–8308.

Möhler, O., P. J. DeMott, G. Vali, and Z. Levin (2007), Microbiology and atmospheric processes: The role of biological particles in cloud physics, *Biogeosciences*, *4*, 1059–1071.

Möhler, O., S. Benz, H. Saathoff, M. Schnaiter, R. Wagner, J. Schneider, S. Walter, V. Ebert, and S. Wagner (2008a), The effect of organic coating on the heterogeneous ice nucleation efficiency of mineral dust aerosols, *Environ. Res. Lett.*, *3*(2), 025007, doi:10.1088/1748-9326/3/2/025007.

Möhler, O., D. G. Georgakopoulos, C. E. Morris, S. Benz, V. Ebert, S. Hunsmann, H. Saathoff, M. Schnaiter, and R. Wagner (2008b), Hetero-

geneous ice nucleation activity of bacteria: New laboratory experiments at simulated cloud conditions, *Biogeosciences*, *5*, 1425–1435.

Möhler, O., J. Schneider, S. Walter, A. J. Heymsfield, D. Schmitt, and Z. J. Ulanowski (2008c), How coating layers influence the deposition mode ice nucleation on mineral particles, pp. 1–5 in *15th Int. Conf. Clouds and Precipitation, Int. Comm. on Clouds and Precip.*, Cancun, Mexico.

Morris, C. E., D. G. Georgakopoulos, and D. C. Sands (2004), Ice nucleation active bacteria and their potential role in precipitation, *J. Phys. IV*, *121*, 87–103.

Murphy, D. M., and T. Koop (2005), Review of the vapour pressures of ice and supercooled water for atmospheric applications, *Q. J. R. Meteorol. Soc.*, *131*(608), 1539–1565, doi:10.1256/qj.04.94.

Obata, H., T. Tanaka, H. Kawahara, and T. Tokuyama (1993), Properties of cell-free ice nuclei from ice nucleation-active pseudomonas-fluorescens kuin-1, *J. Ferment. Bioeng.*, *76*, 19–24.

Parks, G. A. (1965), Isoelectric points of solid oxides solid hydroxides and aqueous hydroxo complex systems, *Chem. Rev. (Washington, DC)*, *65*(2), 177–197, doi:10.1021/cr60234a002.

Parsons, M. T., J. Mak, S. R. Lipetz, and A. K. Bertram (2004), Deliquescence of malonic, succinic, glutaric, and adipic acid particles, *J. Geophys. Res.*, *109*, D06212, doi:10.1029/2003JD004075.

Phillips, V. T. J., P. J. DeMott, and C. Andronache (2008), An empirical parameterization of heterogeneous ice nucleation for multiple chemical species of aerosol, *J. Atmos. Sci.*, *65*(9), 2757–2783, doi:10.1175/2007JAS2546.1.

Phillips, V. T. J., C. Andronache, B. Christner, C. E. Morris, D. C. Sands, A. Bansemer, A. Lauer, C. McNaughton, and C. Seman (2009), Potential impacts from biological aerosols on ensembles of continental clouds simulated numerically, *Biogeosciences*, *6*(6), 987–1014, doi:10.5194/bg-6-987-2009.

Pouleur, S., C. Richard, J. G. Martin, and H. Antoun (1992), Ice nucleation activity in fusarium-acuminatum and fusarium-avenaceum, *Appl. Environ. Microbiol.*, *58*, 2960–2964.

Pratt, K. A., P. J. DeMott, J. R. French, Z. Wang, D. L. Westphal, A. J. Heymsfield, C. H. Twohy, A. J. Prenni, and K. A. Prather (2009), In situ detection of biological particles in cloud ice-crystals, *Nat. Geosci.*, *2*(6), 397–400, doi:10.1038/ngeo521.

Prenni, A. J., M. D. Petters, S. M. Kreidenweis, C. L. Heald, S. T. Martin, P. Artaxo, R. M. Garland, A. G. Wollny, and U. Poschl (2009), Relative roles of biogenic emissions and Saharan dust as ice nuclei in the Amazon basin, *Nat. Geosci.*, *2*(6), 401–404, doi:10.1038/ngeo517.

Pruppacher, H. R., and J. D. Klett (1997) *Microphysics of Clouds and Precipitation*, Kluwer Academic Publishers, Dordrecht, Netherlands.

Rozalen, M., P. V. Brady, and F. J. Huertas (2009), Surface chemistry of K-montmorillonite: Ionic strength, temperature dependence and dissolution kinetics, *J. Colloid Interface Sci.*, *333*(2), 474–484, doi:10.1016/j.jcis.2009.01.059.

Salam, A., U. Lohmann, and G. Lesins (2007), Ice nucleation of ammonia gas exposed montmorillonite mineral dust particles, *Atmos. Chem. Phys.*, *7*, 3923–3931.

Sassen, K. (2002), Indirect climate forcing over the western US from Asian dust storms, *Geophys. Res. Lett.*, *29*(10), 1465, doi:10.1029/2001GL014051.

Sassen, K., P. J. DeMott, J. M. Prospero, and M. R. Poellot (2003), Saharan dust storms and indirect aerosol effects on clouds: CRYSTAL-FACE results, *Geophys. Res. Lett.*, *30*(12), 1633, doi:10.1029/2003GL017371.

Shaw, S. A., D. Peak, and M. J. Hendry (2009), Investigation of acidic dissolution of mixed clays between pH 1.0 and –3.0 using Si and Al X-ray absorption near edge structure, *Geochim. Cosmochim. Acta*, *73*(14), 4151–4165, doi:10.1016/j.gca.2009.04.004.

Shilling, J. E., T. J. Fortin, and M. A. Tolbert (2006), Depositional ice nucleation on crystalline organic and inorganic solids, *J. Geophys. Res.*, *111*, D12204, doi:10.1029/2005JD006664.

Stumm, W. (1992) *Chemistry of the Solid-Water Interface*, Willey-Interscience, New York.

Sullivan, R. C., S. A. Guazzotti, D. A. Sodeman, and K. A. Prather (2007), Direct observations of the atmospheric processing of Asian mineral dust, *Atmos. Chem. Phys.*, *7*, 1213–1236.

Szyrmer, W., and I. Zawadzki (1997), Biogenic and anthropogenic sources of ice-forming nuclei: A review, *Bull. Am. Meteorol. Soc.*, *78*(2), 209–228, doi:10.1175/1520-0477(1997)078<0209:BAASOI>2.0.CO;2.

Tabazadeh, A., E. J. Jensen, and O. B. Toon (1997), A model description for cirrus cloud nucleation from homogeneous freezing of sulfate aerosols, *J. Geophys. Res.*, *102*, 23,845–23,850.

Tabazadeh, A., S. T. Martin, and J. S. Lin (2000), The effect of particle size and nitric acid uptake on the homogeneous freezing of aqueous sulfuric acid particles, *Geophys. Res. Lett.*, *27*, 1111–1114.

Twohy, C. H., and M. R. Poellot (2005), Chemical characteristics of ice residual nuclei in anvil cirrus clouds: Evidence for homogeneous and heterogeneous ice formation, *Atmos. Chem. Phys.*, *5*, 2289–2297.

Usher, C. R., A. E. Michel, and V. H. Grassian (2003), Reactions on mineral dust, *Chem. Rev. (Washington, DC)*, *103*(12), 4883–4939, doi:10.1021/cr020657y.

Vali, G. (1971), Quantitative evaluation of experimental results on heterogeneous freezing nucleation of supercooled liquids, *J. Atmos. Sci.*, *28*(3), 402–409, doi:10.1175/1520-0469(1971)028<0402:QEOERA>2.0.CO;2.

Viani, A., A. F. Gaultieri, and G. Artioli (2002), The nature of disorder in montmorillonite by simulation of X-ray powder patterns, *Am. Mineral.*, *87*, 966–975.

Ward, P. J. D., and P. J. DeMott (1989), Preliminary experimental evaluation of Snomax Snow Inducer, *Pseudomonas syringae*, as an artificial ice nucleus for weather modification, *J. Weather Modification*, *21*, 9–13.

Wiacek, A., and T. Peter (2009), On the availability of uncoated mineral dust ice nuclei in cold cloud regions, *Geophys. Res. Lett.*, *36*, L17801, doi:10.1029/2009GL039429.

Wolber, P. K., C. A. Deininger, M. W. Southworth, J. Vandekerckhove, M. Vanmontagu, and G. J. Warren (1986), Identification and purification of a bacterial ice-nucleation protein, *Proc. Natl. Acad. Sci. USA*, *83*, 19, 7256–7260.

Wood, S. E., M. B. Baker, and B. D. Swanson (2002), Instrument for studies of homogeneous and heterogeneous ice nucleation in free-falling supercooled water droplets, *Rev. Sci. Instrum.*, *73*(11), 3988–3996, doi:10.1063/1.1511796.

Yin, L. J., M. L. Chen, S. S. Tzeng, T. K. Chiou, and S. T. Jiang (2005), Properties of extracellular ice-nucleating substances: From *Pseudomonas fluorescens* MACK-4 and its effect on the freezing of some food materials, *Fish. Sci. (Tokyo)*, *71*, 941–947.

Zobrist, B., C. Marcolli, T. Peter, and T. Koop (2008), Heterogeneous ice nucleation in aqueous solutions: The role of water activity, *J. Phys. Chem. A*, *112*(17), 3965–3975, doi:10.1021/jp7112208.

Zuberi, B., A. K. Bertram, C. A. Cassa, L. T. Molina, and M. J. Molina (2002), Heterogeneous nucleation of ice in $(NH_4)_2SO_4$-$H_2O$ particles with mineral dust immersions, *Geophys. Res. Lett.*, *29*(10), 1504, doi:10.1029/2001GL014289.

A. K. Bertram and D. I. Chernoff, Department of Chemistry, University of British Columbia, Vancouver, BC, Canada, V6L 2Y6. (bertram@chem.ubc.ca)